

General Disclaimer

One or more of the Following Statements may affect this Document

- This document has been reproduced from the best copy furnished by the organizational source. It is being released in the interest of making available as much information as possible.
- This document may contain data, which exceeds the sheet parameters. It was furnished in this condition by the organizational source and is the best copy available.
- This document may contain tone-on-tone or color graphs, charts and/or pictures, which have been reproduced in black and white.
- This document is paginated as submitted by the original source.
- Portions of this document are not fully legible due to the historical nature of some of the material. However, it is the best reproduction available from the original submission.

**NASA TECHNICAL
MEMORANDUM**

NASA TM X-52648

NASA TM X-52648

**SUMMARY OF VARIABLE PROPERTY HEAT-TRANSFER EQUATIONS
AND THEIR APPLICABILITY TO A NUCLEAR ROCKET NOZZLE**

by Maynard F. Taylor
Lewis Research Center
Cleveland, Ohio

TECHNICAL PAPER proposed for presentation at
Fourth International Heat Transfer Conference
Versailles/Paris, France, August 31-September 5, 1970



N70-23452

(ACCESSION NUMBER)	(THRU)
<i>16</i>	<i>1</i>
(PAGES)	(CODE)
<i>NASA-TM X-52648</i>	<i>33</i>
(NASA CR OR TMX OR AD NUMBER)	(CATEGORY)

FACILITY FORM 802

SUMMARY OF VARIABLE PROPERTY HEAT-TRANSFER EQUATIONS
AND THEIR APPLICABILITY TO A NUCLEAR ROCKET NOZZLE

by Maynard F. Taylor

Lewis Research Center
Cleveland, Ohio

TECHNICAL PAPER proposed for presentation at

Fourth International Heat Transfer Conference
Versailles/Paris, France, August 31-September 5, 1970

NATIONAL AERONAUTICS AND SPACE ADMINISTRATION

SUMMARY OF VARIABLE PROPERTY HEAT-TRANSFER EQUATIONS AND
THEIR APPLICABILITY TO A NUCLEAR ROCKET NOZZLE

Maynard F. Taylor
NASA Lewis Research Center, Cleveland, Ohio

Abstract

The prediction equation resulting from a thorough study of all available single-phase hydrogen heat-transfer data is modified to predict heat-transfer coefficients on both the concave and convex surface of curved tubes. The prediction equations for straight and curved tubes are then applied to the Phoebus-2 nuclear rocket nozzle. Predicted exit pressure and temperatures are compared with experimental values from recent nuclear tests of the Phoebus-2 nozzle, and found to be in very good agreement.

INTRODUCTION

The extreme conditions encountered in regeneratively cooled nuclear rocket nozzles produce severe heat-transfer problems in the coolant passages. An effective method of predicting heat-transfer coefficients in the cooling passages is essential to the optimization of any nozzle design. Of particular concern is the high heat flux throat region fluxes of 20 Btu per second per square inch (32.7 megawatts per square meter) and higher are reached.

The author of this paper has previously studied all available single-phase hydrogen heat transfer for flow through straight tubes and recommended a single correlation equation for a wide range of conditions [1]. In the present paper the calculated heat transfer coefficients are shown to be in very close agreement with recent experimental values reported in [2]. More recently the author has modified the straight tube equation to include the effects of curvature from [3]. The modified equation is compared with some existing experimental data from single curved tubes [4]. These results and recommended applications of the equations have been reported by this author [5].

Of course, the most severe test of the ability of these equations to calculate heat transfer in the cooling passages of a nuclear rocket nozzle is to compare the predictions with experimental results. In this paper the predictions are compared with the results obtained from recent nuclear tests of the Phoebus-2 nuclear rocket nozzle.

HEAT-TRANSFER COEFFICIENTS IN STRAIGHT TUBES

A study of 4622 experimentally determined hydrogen heat-transfer coefficient data points [1] resulted in the following prediction equation:

$$Nu = 0.023 Re_b^{0.8} Pr_b^{0.4} \left(\frac{T_w}{T_b} \right)^{-C_1} \quad (1)$$

where

$$C_1 = \left(0.57 - \frac{1.59}{x/D} \right)$$

for the range of inlet pressure and inlet temperature shown in figure 1. The use of the temperature-entropy diagram is a convenient method of showing the location of measured inlet pressure and temperature in relation to the saturation lines and critical pressure p_c and critical temperature T_c .

The hydrogen data are separated into regions 1 and 2 as shown in figure 1. These regions are the result of the study of the effect of inlet temperature T_i , inlet pressure p_i , and the transposed critical temperature (the temperature at which the specific heat at constant pressure reaches a maximum) T^* . In region 1, 87 percent of the 3674 heat-transfer coefficients predicted by equation (1) deviates less than ± 25 percent from the measured values. Region 2 is defined by $45^\circ R < T_i < T^*$ and $p_c < p_i < 530$ psia and is often referred to as the near-critical region. In region 2, 40 percent of the 948 predicted heat-transfer coefficients deviates less than ± 25 percent from the measured values. At present, there is considerable doubt about the transport properties in this region.

Equation (1) is used to predict heat-transfer coefficients which can be compared to the most recent experimental data for the range of conditions encountered in nuclear rocket nozzles. The ratio of these predicted coefficients to the measured values is shown as a function of the ratio of wall to fluid bulk temperatures in figure 2. Figure 2 shows that 94 percent of the heat-transfer coefficients predicted using equation (1) deviated less than ± 20 percent from the measured values.

HEAT-TRANSFER COEFFICIENTS IN SYMMETRICALLY HEATED CURVED TUBES

Heat-transfer measurements have been reported for both the concave or "swept" side and the convex or "unswept" side of curved circular tubes [4]. Equation (1) was first tried without any change from the form that correlated straight tube data to predict heat-transfer coefficients for both the concave and convex sides of the symmetrically heated test sections. The ratio of the heat-transfer coefficient predicted by equation (1) to the measured coefficient is shown as a function of temperature ratio in figure 3. As might be expected, the predicted heat-transfer coefficient is lower than the measured value on the concave side and higher than the measured value on the convex side. The calculated heat-transfer coefficient is as small as one-half the experimental value on the concave side and as large as almost twice the experimental value on the convex side.

Equation (1) is modified [5] with the $It\bar{o}$ correction factor for curvature [3] to give the equation

$$Nu_b = 0.023 Re_b^{0.8} Pr_b^{0.4} \left(\frac{T_w}{T_b} \right)^{-C_1} \left[Re_b \left(\frac{r}{R} \right)^2 \right]^{0.05} \quad (2)$$

for the concave side.

The convex side of a curved tube is rarely given any consideration, but in reference [5] the reciprocal of the $It\bar{o}$ factor was used to modify equation (1) to give

$$Nu_b = 0.023 Re_b^{0.8} Pr_b^{0.4} \left(\frac{T_w}{T_b} \right)^{-C_1} \left[Re_b \left(\frac{r}{R} \right)^2 \right]^{-0.05} \quad (3)$$

for the convex side.

The results of using equations (2) and (3) to predict the heat-transfer coefficients on the concave and convex sides of a tube are shown in figures 4(a) and (b), respectively. The experimental data in figure 4 is the same data used in figure 3. Approximately 90 percent of the predicted heat-transfer coefficients deviated less than ± 20 percent from the experimental values.

It appears that the $It\bar{o}$ correction does improve the correlation and that equations (2) and (3) will predict heat-transfer coefficients on the concave and convex sides of curved tubes, respectively.

ASYMMETRICALLY HEATED CURVED TUBES

Both the straight and curved tube data presented up to this point are for symmetrically heated circular tubes. In the rocket nozzle the cooling passages are noncircular and they are heated from only one side. Some single tube data are available for asymmetrically heated circular and noncircular passages curved to simulate the throat and high flux region of the Phoebus-2 nozzle [2]. Heat-transfer coefficients predicted by equation (2) were compared to these experimental values for conditions as near as possible to those for the actual nozzle.

Figure 5 shows the ratio of the heat-transfer coefficients calculated by equation (2) to the experimental coefficients as a function of the dimensionless distance from the entrances. Figure 5 shows the ratio of coefficients for the Phoebus-2 contour. The agreement between predicted and measured heat-transfer coefficients is good for single, asymmetrical, curved tubes that simulate the Phoebus-2 geometry.

An important use of the heat-transfer coefficient is in the prediction of wall temperatures. Equation (2) is used to predict the inside wall temperatures which are compared with the measured wall temperatures [2] in figure 6 for the simulated Phoebus-2 coolant tube. The agreement is good and the prediction is conservative which is desirable.

APPLICATION OF PREDICTION EQUATIONS TO ROCKET NOZZLES

Regeneratively cooled rocket nozzles are made up of noncircular passages formed to give the desired area ratios, and are essentially combinations of straight and curved tubes. The success demonstrated in predicting heat-transfer coefficients in straight tubes using equation (1) and curved tubes using equations (2) and (3) encourages the use of these equations in predicting heat transfer coefficients in the coolant passages of a rocket nozzle.

To predict the heat-transfer coefficients in the cooling passage of a nozzle, the following equations are recommended [5].

Entrance of Coolant Passage

Straight entrance $x/D > 1$

$$Nu_b = 0.023 Re_b^{0.8} Pr_b^{0.4} \left(\frac{T_w}{T_b} \right)^{-C_1} \quad (1)$$

90° angle bend and orifice entrance $x/D > 5$

$$Nu_b = 0.023 Re_b^{0.8} Pr_b^{0.4} \left(\frac{T_w}{T_b} \right)^{-C_1} \left(1 + F_1 \frac{D}{x} \right) \quad (4)$$

where $F_1 = 5$ for a 90° angle bend and 11 for an orifice entrance. The term $(1 + F_1(D/x))$ has been previously reported [6].

Throat section (concave curvature)

$$Nu_b = 0.023 Re_b^{0.8} Pr_b^{0.4} \left(\frac{T_w}{T_b} \right)^{-C_1} \left[Re_b \left(\frac{r}{R} \right)^2 \right]^{0.05} \quad (2)$$

Exit section (convex curvature)

$$Nu_b = 0.023 Re_b^{0.8} Pr_b^{0.4} \left(\frac{T_w}{T_b} \right)^{-C_1} \left[Re_b \left(\frac{r}{R} \right)^2 \right]^{-0.05} \quad (3)$$

Any straight sections

$$Nu_b = 0.023 Re_b^{0.8} Pr_b^{0.4} \left(\frac{T_w}{T_b} \right)^{-C_1} \quad (1)$$

At present it is not known how far the effects of curvature on the heat-transfer coefficient will extend downstream of the point of tangency where a curved tube becomes straight. It is reasonable to assume that the effect of curvature would diminish with x/D rather than change abruptly at the point of tangency. The curvature effect appears to be present at the last instrumented station shown in figure 6(b) which is 2 diameters downstream of the tangency point. In the calculations presented in this paper the effects of curvature was assumed to begin or end at the point of tangency with the straight sections.

COMPARISON OF PREDICTED RESULTS WITH PHOEBUS-2 NUCLEAR TESTS

A severe test of the prediction equations proposed in this investigation is to use them to predict the heat-transfer in the coolant passages of the Phoebus-2 nuclear rocket nozzle. The Phoebus-2 nozzle was run at the highest power level ever achieved by a nuclear rocket engine, 4080 megawatts. The conditions for a wide range of tests are shown in table I. The equations presented herein were used to revise the coolant side heat-transfer calculations in an existing digital computer program [7] for calculating heat transfer and fluid flow for convectively cooled rocket nozzles.

The calculation of heat transfer from the hot propellant is also necessary and the Nusselt equation:

$$Nu_f = C_g Re_f^{0.8} Pr_f^{0.3} \quad (5)$$

is used in the computer program. Common practice [7] is to use a gas coefficient, C_g , that is a function of nozzle area ratio. In this investigation both a constant C_g of 0.026 and an empirically determined variable C_g provided by the Aerojet General Corp. are used and the results compared. The variable C_g and the area ratio for the 34 stations in the nozzle is shown in table II. There is no provision in the computer program for the small amount of film cooling on the hot-gas side of the chamber wall. The maximum effect can be estimated by assuming no heat addition at the last 4 stations (about 12.5 in. or 32 cm).

Both friction and momentum pressure drops in the coolant passages were calculated in the computer program. The equation used to calculate these pressure drops in the program were not changed. The pressure drop is affected by the coolant temperature, thus making temperature rise and pressure drop inter-related.

Total temperature and static pressure of the coolant at each axial station for test EP IV-6 are calculated and shown in figure 7. The only measured values for comparison are the coolant passage exit temperature and pressure, which are also shown in figure 7. The solid line represents the calculated values with C_g varying as shown in table III. The dashed line represents the calculated values using a constant C_g of 0.026. The agreement between both calculated values and the measured values is very good. The measured and calculated exit pressures and temperatures and percent deviation for several other EP-IV tests are shown in table III. For the case of no heat addition in the last four stations (corresponding to film cooling of the chamber wall) both the exit temperature and pressure fell within the range of accuracy of the measured values and are not shown in table III.

In figure 8 the local hot-gas side wall temperature and the local coolant side heat flux is shown as a function of axial position. The solid line represents the values calculated using the variable C_g from table III and the dashed line represents the values resulting from the use of a constant C_g of 0.026. The greatest differences resulting from the calculations using the different C_g 's are in the chamber. The use of temperature rise and pressure drop measurements indicates little of what happens locally in a rocket nozzle. Wall temperature and heat flux did not vary as much in the throat region as they did in the nozzle chamber. This is expected since the C_g in table II is two to three times the constant value of 0.026.

The good agreement between the two sets of calculations and the measured exit temperature and pressure indicates that with accurate predictions on the coolant side the hot-gas side equations are of secondary importance in predicting exit conditions. However, as one might expect, local wall temperatures and heat flux are very much affected by local gas-side heat-transfer coefficients.

The rather abrupt changes in wall temperature is due to the application of the curvature correction which increased the heat-transfer coefficient on the concave or swept surface (decreasing the wall temperature) and decreased the heat-transfer coefficient on the convex or unswept surface (increasing the wall temperature). In the actual nozzle wall these changes might not be so abrupt because of axial heat conduction in the coolant passage wall. Axial heat conduction was not accounted for in the computer program.

CONCLUDING REMARKS

The computer program for calculating heat transfer and fluid flow in regeneratively cooled rocket nozzles [7] was revised to include the heat-transfer prediction equations recommended in this investigation. The revised program was then used to predict exit temperatures and pressures, nozzle wall temperatures, and heat flux to the coolant. Only the exit temperature and pressures from the Phoebus-2 nuclear tests were available for comparison with predicted values. Two sets of calculations were made for each nuclear test: one in which the gas constant C_g was constant at 0.026, and another test which used recommended C_g 's that varied from 0.018 to 0.080. Both sets of calculations yielded exit temperatures and pressures that are in good agreement with measured values. This indicates that with accurate predictions on the coolant side, the less well developed heat-transfer correlations on the hot-gas side are of secondary importance in predicting total temperature rise and static pressure drop. The hot-gas side heat-transfer does, however, change the wall temperature distribution. This indicates that measured local wall temperatures are needed to verify any hot-gas side equations. The good agreement between measured and calculated exit temperature and pressure does not necessarily mean that all the heat-transfer and fluid flow problems of regeneratively cooled rocket engines are now solved. Instead, it indicates a need for work on the hot-gas side and a need for local wall temperature and coolant pressure measurements. Such measurements for any rocket engine test, especially a nuclear engine, presents a considerable challenge to present technology.

NOMENCLATURE

C	coefficient in Nusselt equation	T^*	transposed critical temperature (temperature at which specific heat of fluid at constant pressure reaches a maximum)
c_p	specific heat of gas at constant pressure	v	velocity
D	inside diameter of test section	x	distance from entrance of test section
G	mass flow rate per unit cross- sectional area	μ	absolute viscosity of gas
h	local heat-transfer coefficient	ρ	density of gas
k	thermal conductivity of gas	Subscripts:	
Nu	Nusselt number, hD/k	b	bulk (when applied to properties, indicates evaluation at bulk temperature T_b)
Pr	Prandtl number, $c_p\mu/k$	c	critical
p	absolute static pressure	f	film (when applied to properties indicates evaluation at film temperature T_f)
q	rate of heat transfer to gas per unit area	g	gas-side
R	radius of curvature	i	inlet
Re_b	bulk Reynolds number, GD/μ_b	w	wall
Re_f	modified film Reynolds number, $\rho_f V_b D / \mu_f$		
r	inside radius of passage		
T	temperature		

REFERENCES

- [1] M. F. Taylor: Correlation of Local Heat-Transfer Coefficients for Single-Phase Turbulent Flow of Hydrogen in Tubes with Temperature Ratios to 23. NASA Tech. Note D-4332 (1968).
- [2] Anon.: Heat Transfer to Cryogenic Hydrogen Flowing Turbulently in Straight and Curved Tubes at High Heat Fluxes. NASA CR-678, (1967).
- [3] H. Itō: Friction Factors for Turbulent Flow in Curved Pipes. J. Basic Eng., vol. 81, No. 2, p. 123/134 (1959).
- [4] W. D. Stinnett: An Experimental Investigation of the Heat Transfer to Hydrogen at Near Critical Temperatures and Supercritical Pressures Flowing Turbulently in Straight and Curved Tubes. Rept. 2551 (NASA CR-50836), Aerojet-General Corp. (1963).
- [5] M. F. Taylor: Heat-Transfer Predictions in the Cooling Passages of Nuclear Rocket Nozzles. J. Spacecraft Rockets, vol. 5, No. 11, p. 1353/1355 (1968).
- [6] L. M. K. Boelter, G. Young, and H. W. Iverson: An Investigation of Aircraft Heaters - XXVII. Distribution of Heat Transfer Rate in the Entrance Section of a Circular Tube. NACA Tech. Note 1451 (1948).
- [7] J. E. Rohde, R. A. Duscha, and G. Derderian: Digital Codes for Design and Evaluation of Convectively Cooled Rocket Nozzle with Application to Nuclear-Type Rocket. NASA Tech. Note D-3798 (1967).

TABLE I. - OPERATING CONDITIONS FOR PHOEBUS 2A EP-IV NUCLEAR ROCKET TESTS^a

(a) U. S. Customary Units

Test	Flow rate, lbm/sec		Chamber conditions		Nozzle inlet conditions		Thermal power, MW
	Hot gas	Coolant	Pressure, psia	Temperature, °R	Pressure, psia	Temperature, °R	
1	108.6	97.9	124	1240	197	40.8	490
2	142.0	125.6	214	2120	362	43.0	1090
3	192.2	176.6	351	3080	650	47.2	2190
4	244.1	219.8	435	2940	820	50.9	2650
5	245.2	219.5	506	3890	975	52.1	3630
6	262.3	234.9	555	4660	1080	53.9	4080

(b) S. I. Units

Test	Flow rate, kg/sec		Chamber conditions		Nozzle inlet conditions		Thermal power, MW
	Hot gas	Coolant	Pressure, MN/m ²	Temperature, K	Pressure, MN/m ²	Temperature, K	
1	49.3	44.4	0.855	689	1.36	22.6	490
2	64.4	57.0	1.48	1178	2.50	23.9	1090
3	87.2	80.1	2.42	1711	4.48	26.2	2190
4	110.7	99.7	3.00	1633	5.65	28.3	2650
5	111.2	99.6	3.49	2161	6.72	28.9	3630
6	119.0	106.6	3.83	2256	7.45	29.9	4080

^a Unpublished data received from Donald L. Hanson, Los Alamos Scientific Laboratory.

TABLE II. - AREA RATIO AND GAS COEFFICIENT
FOR EACH CALCULATION STATION^a

Region	Station	Area ratio	Gas coefficient, C_g	Region	Station	Area ratio	Gas coefficient, C_g
Divergent	1	7.00	0.032	Convergent	21	2.34	0.027
	2	6.44	.033		22	3.17	.028
	3	5.90	.033		23	4.13	.028
	4	5.39	.033		24	5.21	.029
	5	4.90	.034		25	6.42	.032
	6	4.43	↓		26	7.76	.035
	7	3.98			27	9.22	.038
	8	3.56		Knuckle	28	10.81	0.042
	9	3.17			29	11.85	.045
	10	2.79			30	12.22	.048
	11	2.44	Chamber	31	12.22	0.056	
	12	2.12		.032	32	↓	.064
	13	1.81		.030	33		.075
	14	1.53		.028	34		.080
	15	1.28		.024			
Throat	16	1.04	0.018				
	17	1.00	.018				
	18	1.07	.028				
	19	1.27	.029				
	20	1.63	.029				

^aUnpublished data received from James O. Sane, Aerojet-General Corp.

TABLE III. - CALCULATED AND MEASURED TEMPERATURES AND PRESSURES
AT EXIT OF COOLANT PASSAGES FOR PHOEBUS 2A EP-IV TESTS

(a) U. S. Customary Units

Test EP-IV	Measured exit tem- perature, T_m' °R (a)	Gas coefficient			Measured exit pres- sure, P_m' psi (a)	Gas coefficient		
		from table II		$C_g = 0.026$		from table II		$C_g = 0.026$
		Calculated exit tem- perature, T_c' °R	$\frac{T_c - T_m}{T_m} \times 100$, percent	Calculated exit tem- perature, T_c' °R		Calculated exit pres- sure, P_c' psi	$\frac{P_c - P_m}{P_m} \times 100$, percent	Calculated exit pres- sure, P_c' psi
1	71	59	-17	59	168	176	4.8	167
2	75	74	-1.3	69	296	288	-2.7	298
3	95	102	7.4	91	499	483	-3.2	502
4	96	103	7.3	93	616	593	-3.7	614
5	124	131	5.6	117	720	701	-2.6	729
6	136	137	5.4	122	790	769	-2.7	799

(b) S. I. Units

Test EP-IV	Measured exit tem- perature, T_m' K (a)	Gas coefficient			Measured exit pres- sure, P_m' MN/m ² (a)	Gas coefficient		
		from table II		$C_g = 0.026$		from table II		$C_g = 0.026$
		Calculated exit tem- perature, T_c' K	$\frac{T_c - T_m}{T_m} \times 100$, percent	Calculated exit tem- perature, T_c' K		Calculated exit pres- sure, P_c' MN/m ²	$\frac{P_c - P_m}{P_m} \times 100$, percent	Calculated exit pres- sure, P_c' MN/m ²
1	39	33	-17	33	1.16	1.21	4.8	1.15
2	42	41	-1.3	38	2.04	1.99	-2.7	2.05
3	53	57	7.4	51	3.44	3.33	-3.2	3.46
4	53	57	7.3	52	4.25	4.09	-3.7	4.23
5	69	73	5.6	65	4.96	4.83	-2.6	5.03
6	72	76	5.4	68	5.45	5.30	-2.7	5.51

^aUnpublished data received from Donald L. Hanson, Los Alamos Scientific Laboratory.

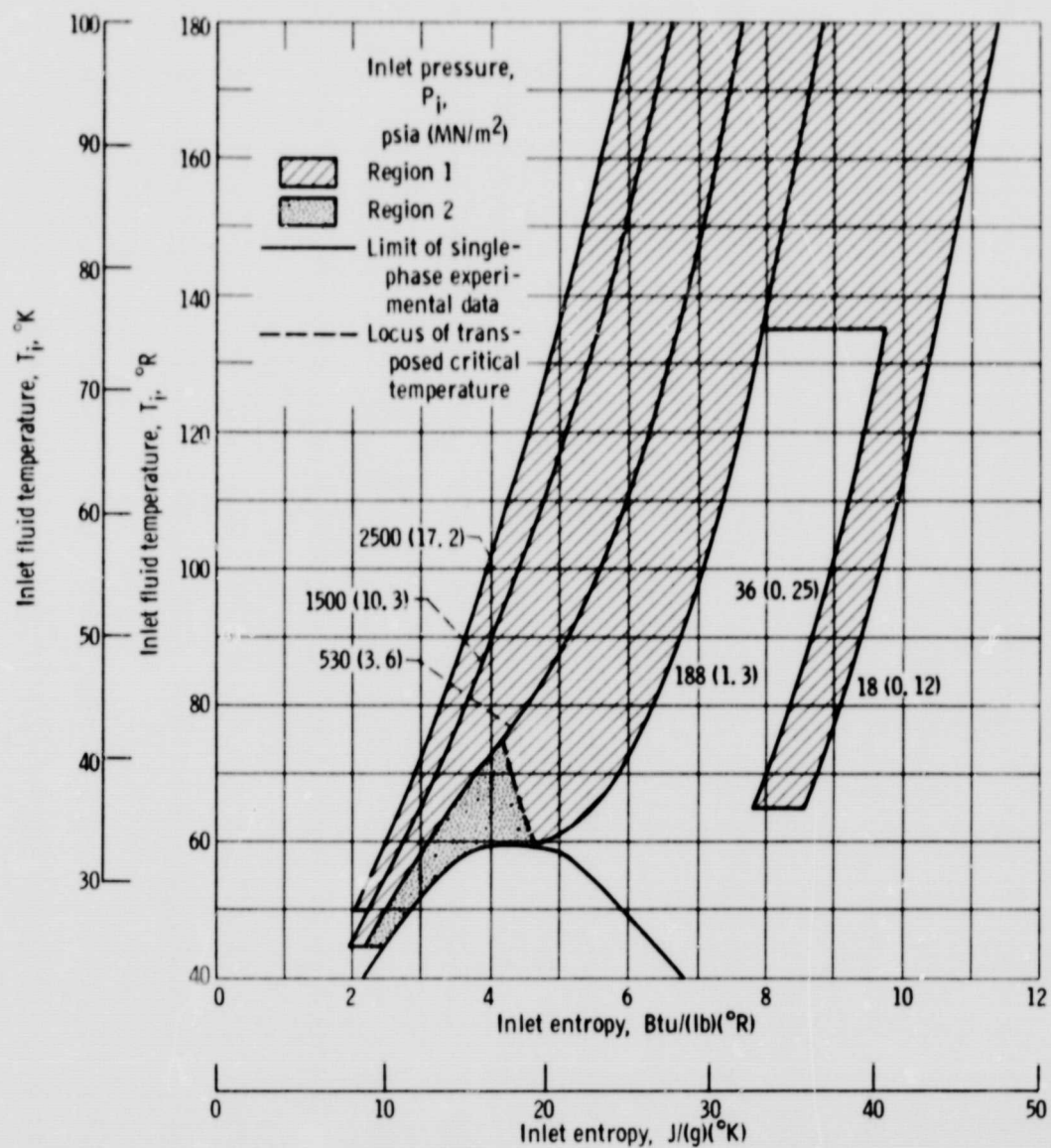


Figure 1. - Range of hydrogen inlet temperature and inlet pressure for which equation (1) has been experimentally checked.

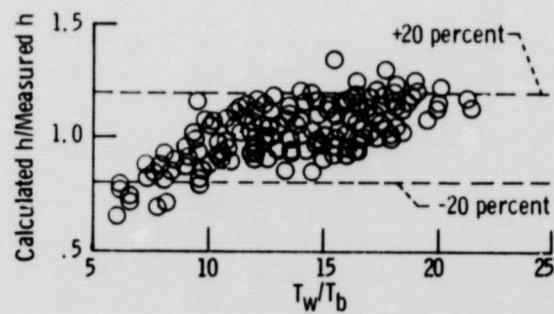


Figure 2. - Variation of the ratio of calculated to measured heat transfer coefficients with temperature ratio. Straight tube data [2].

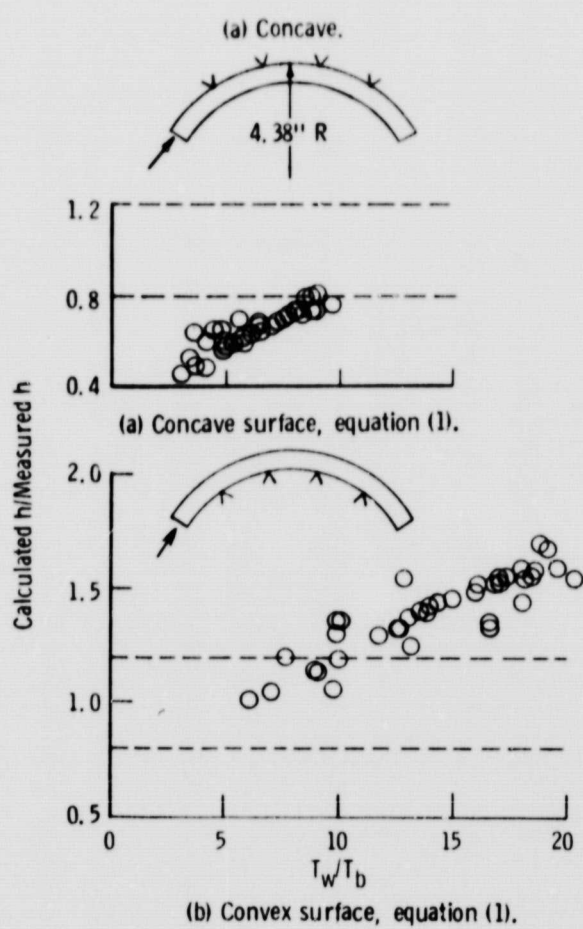


Figure 3. - Variation of the ratio of calculated to measured heat transfer coefficients with temperature ratio. Data from symmetrically heated curved tubes [4].

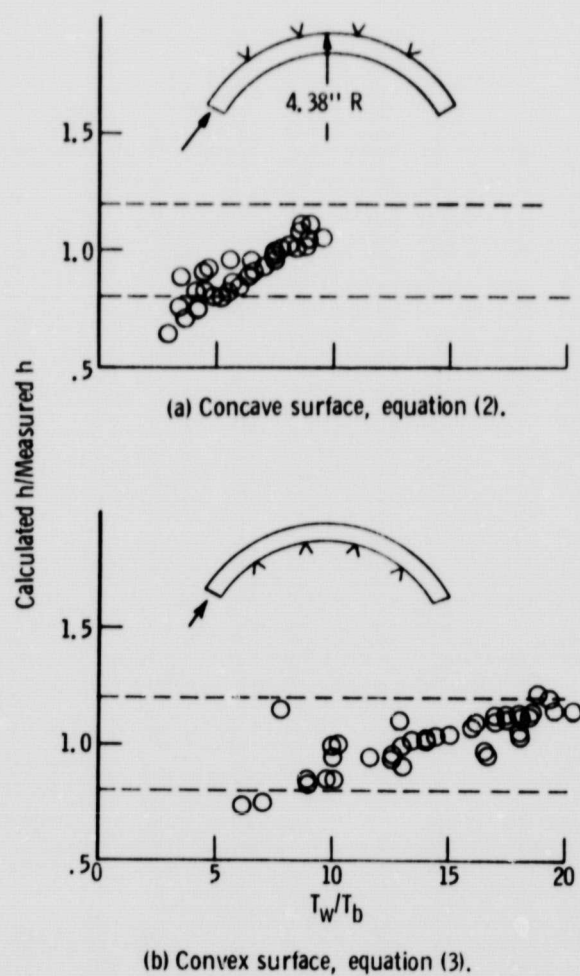


Figure 4. - Variation of the ratio of calculated to measured heat transfer coefficients with temperature ratio. Data from symmetrically heated curved tubes [4].

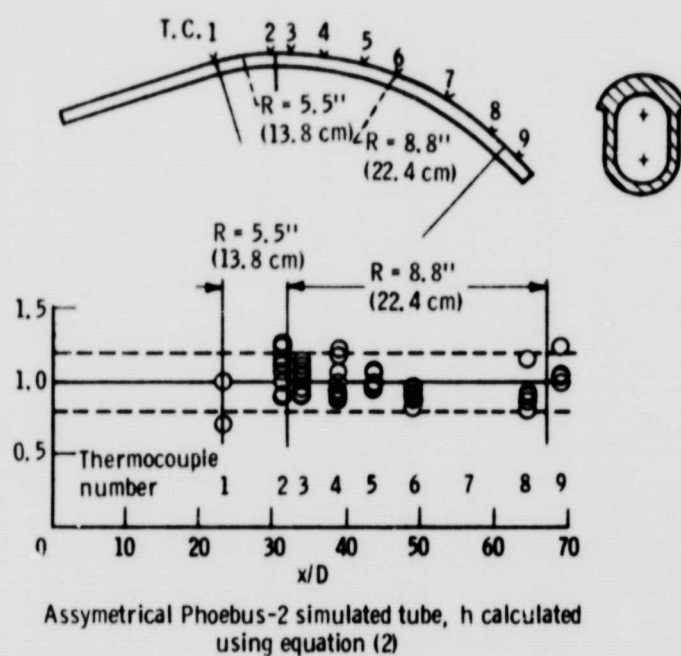


Figure 5. - Variation of the ratio of calculated to measured heat transfer coefficients with axial distance from entrance. Data from asymmetrically heated curved tube [2].

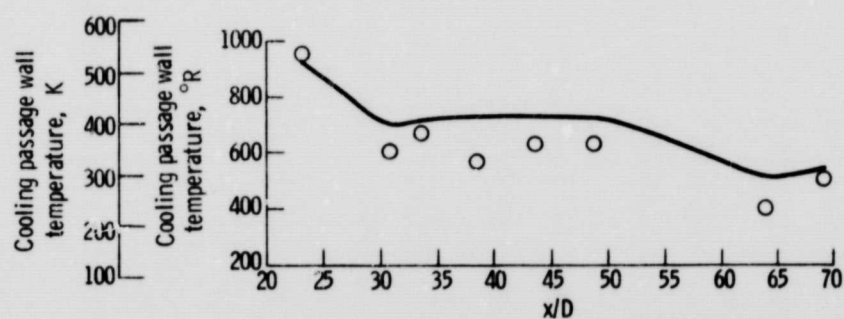


Figure 6. - Variation of inside wall temperature with axial distance from entrance for the Phoebus-2 contour [2].

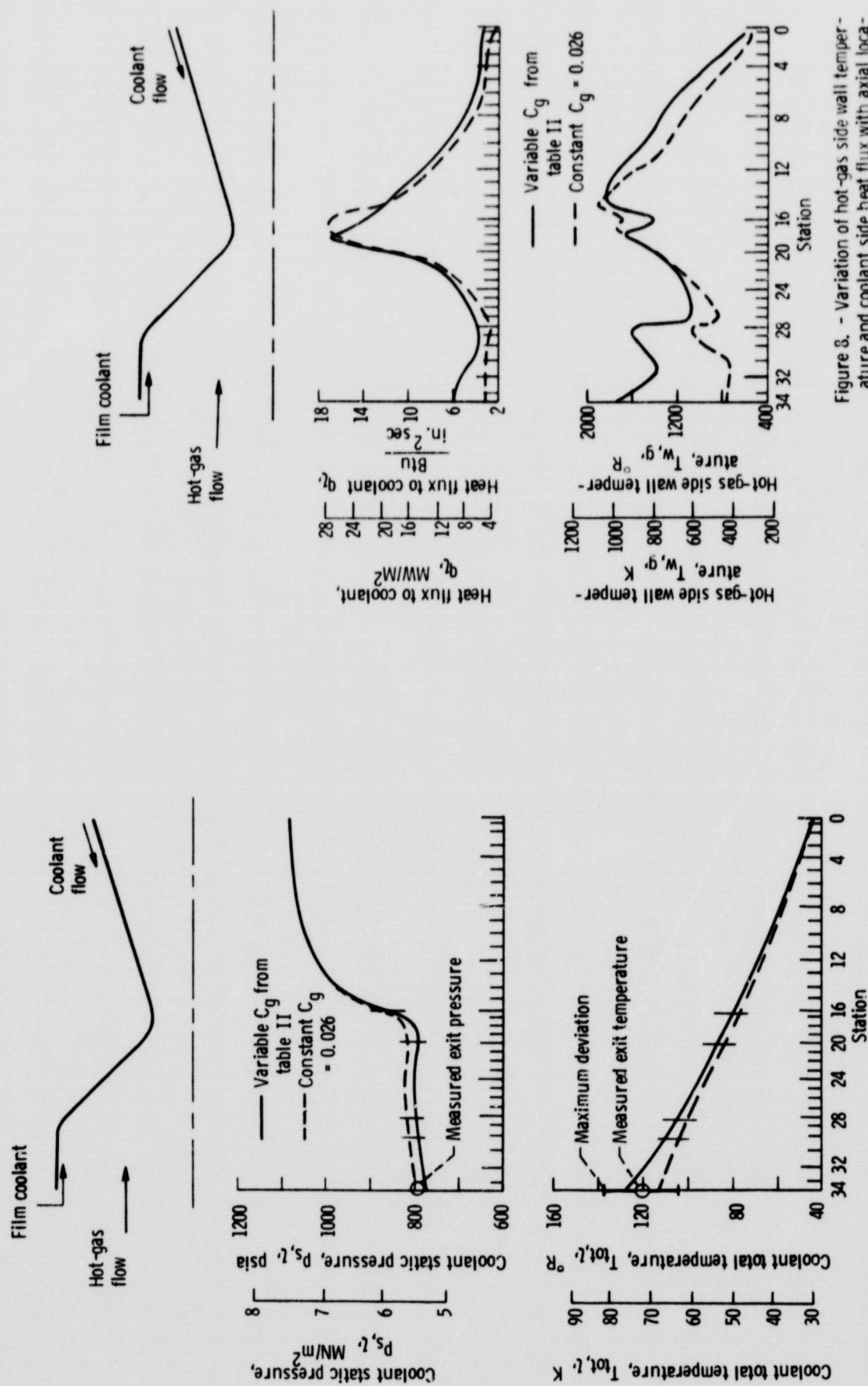


Figure 7. - Variation of coolant total temperature and static pressure with axial location. Thermal power 4080 megawatts.

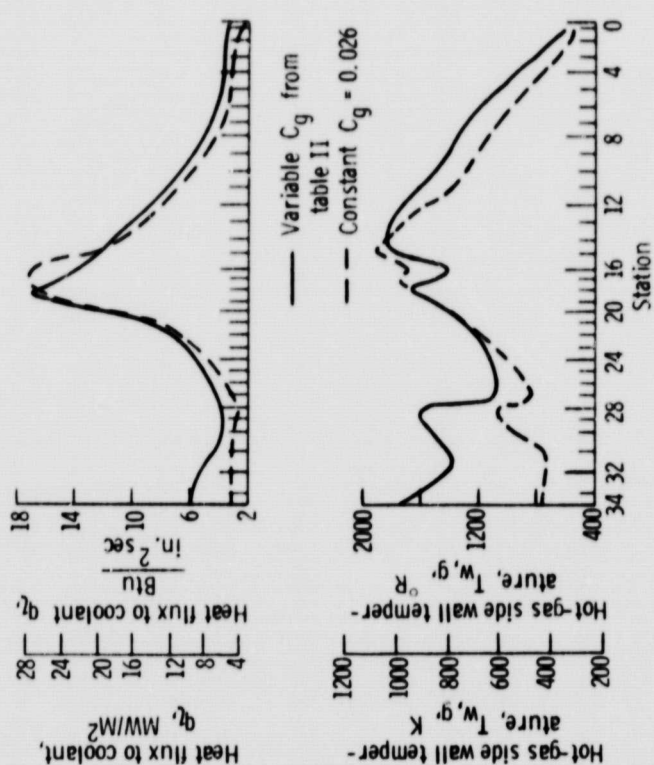


Figure 8. - Variation of hot-gas side wall temperature and coolant side heat flux with axial location. Thermal power, 4080 megawatts.